

Sound velocity predictions in refrigerant mixtures

Martin Doubek¹

¹ Department of Physics, Faculty of mechanical engineering, Czech Technical University in Prague, Czech Republic

Abstract

Fluid composition analysis based on speed of sound measurement is an interesting alternative to well established methods such as the infrared spectroscopy or semiconductor sensors. Numerous publications describing broad applications of this method can be found: carbon dioxide concentration monitoring in breathing apparatus, monitoring of lubricant content in refrigerants, analysis of oil in reservoirs, monitoring of recirculating exhaust gases in combustion engine or analysis of Titan's atmosphere by Huygens probe. Department of Applied Physics at the Faculty of Mechanical Engineering of the Czech Technical University in Prague is involved in development of analysers based on speed of sound measurement. Similar research is currently ongoing at CERN. These analysers are employed to analyse refrigerant mixtures (R218+R116), to monitor refrigerants contamination and to serve as leak detectors. The aim of the presented work is to provide flexible and easy-to-use models for accurate speed of sound prediction which will make a further development of the analysers possible. The main incentive behind the current effort is a lack of proven models that could be used for mixtures of unlike components (R218+N₂). Several selected SAFT (Statistical Associating Fluid Theory) models have been compared to data obtained from our own experiments and data gathered from literature. On top of that, the model fitting parameters have been optimized to increase prediction accuracy.

Key words: Speed of sound, composition analysis, equations of state, SAFT

1 Introduction

Sensors based on speed-of-sound measurements have a wide range of applications. Apart from the basic and well-known distance and thickness measurements and liquid level detection, there are some very interesting applications based on fluid analysis from in situ speed-of-sound measurements: lubrication oil quality sensors [1], precise determination of air humidity [2] and temperature [3], and measurements of the oil content in refrigerant flow [4]. Most of these applications make use of a composition analysis of a fluid based on speed-of-sound, pressure and temperature measurements. In general, the analysis can be made either in the liquid phase or in the gas phase, and its applications span from the petrochemical industry [5] through medical instrumentation [6], the food industry [7], even to space exploration [8]. Our attention is directed toward applications in refrigeration: composition analysis of refrigerant blends, detection of impurities and contaminants in refrigerants, and leak detection.

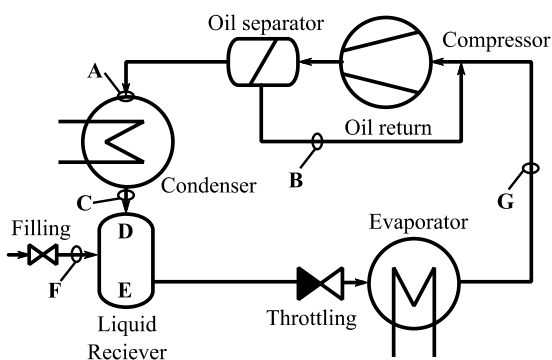


Figure 1. Measurement principle

The simplified refrigeration circuit in Figure 1. shows locations denoted with bold capital letters where a speed-of-sound based sensor can be placed. The sensor in the

given location can monitor: (A) noncondensable gases in the condenser; (B) lubrication oil quality; (C) the oil content in the condenser liquid; (D) the composition of the gas phase in a receiver; (E) the composition of the liquid phase in receiver, (F) the composition of the refrigerant to be filled, and (G) the composition of the returning vapor.



Figure 2. Speed of sound sensor for liquid phase [9]

The major advantage of speed-of-sound based analysis is that it can be carried out in real time. The speed of sound can be measured with uncertainty better than 0.5% with relatively simple and inexpensive instrumentation. Uncertainties well below 0.1% can be achieved even in "field" conditions. A range of sensors and instruments suitable for both gas and liquid phase measurements are commercially available.

An example of commercial speed of sound sensor for liquid phase is shown in the Figure 2. The Rhosonic 8500 Ultrasonic Process Concentration Analyzer [9] employs a time-of-flight measurement technique at sound frequencies from 1 to 7.5 MHz. The sensors can be inserted directly into a flow of liquid in order to provide online measurement and it provides simultaneous measurement of speed of sound, sound attenuation and temperature. An additional conductivity probe is included in some models. A very sophisticated fluid analysis can be carried out based these measured quantities. The measurement accuracy is 0.1% or 0.01 m/s with resolution of 0.002 m/s. The sensor is especially suitable

for food or oil industry.

TTP company from United Kingdom recently developed a miniature low-consumption speed of sound sensors for gases [10], Figure 3. This is only one example from multitude of sensors available for online monitoring of gas concentrations. The measurement accuracy up to 0.001 m/s or 0.01% is common for these devices. One can choose from selection of complete microprocessor-controlled units with display or standalone measurement cells.

Ultrasonic flowmeters, Figure 4., are popular in every industry sector. They are based on speed of sound measurement, however, the speed of sound values are not always available to the user alongside the flow measurements. Apart from the fluid analysis, the speed of sound measured by the flowmeter can be used to detect flowmeter fouling and to determine the quality of the flow measurement in application such is the natural gas transport where heavy fouling can occur.

The most convenient way to execute a composition analysis is at low pressure in well superheated vapor, so that the fluid behavior is close to ideal gas behavior. To determine the concentration, the measured data can be regressed by the well-known ideal gas model with a simple mixing rule. However, this is not always possible. At pressures and temperature close to saturation or in the liquid phase, simple models like the ideal gas equation or cubic-type equations of state are not adequate for the subsequent analysis. High-accuracy multi-parameter equations of state can be used instead. These equations are available for most of the widely-used engineering fluids, and they can be used to predict the speed of sound with high accuracy. Software packages such as NIST REFPROP [12] use various multi-parameter equations to model different fluids. The uncertainty of speed-of-sound prediction is well below 0.1% for gases like argon, nitrogen or carbon dioxide, and below 1% for refrigerants. REFPROP uses different equations of state for different fluids or families of fluids, and it is therefore incapable of predicting the properties of certain mixtures consisting of unlike components (e.g. $N_2+C_3F_8$).



Figure 3. Speed of sound sensor for gas phase [10]

In our research, we evaluate “easy-to-use” models for predicting the speed of sound in pure components and mixtures containing both like and unlike components. We will evaluate models that can be used for the rapid development of novel applications for speed-of-sound based sensors. Many papers have evaluated various thermodynamic models by comparing the predictions of various thermodynamic properties with experimental data or with molecular simulations. A comparison with speed-

of-sound data is frequently included, since high-quality experimental data are available for most of the widely-used fluids. The comparisons are often made over wide ranges of pressures and temperatures, disregarding the typical ranges for engineering applications. Although a certain model may show better average agreement than others over a wide range of experimental data, it is difficult to conclude that this result would be the same for the narrow range for a particular engineering application.



Figure 4. Custom-made ultrasonic flowmeter [11]

2 Selection of models

Models for speed-of-sound predictions can be divided into acoustic models and models based on conventional equations of state. Our primary interest is in models that can be applied to fluorocarbons and their mutual blends, and also their mixtures with other common engineering fluids, such as natural refrigerants (carbon dioxide, propane, etc.), water, oxygen, noble gases and oils. The requirements are in principle very limiting. Models developed specifically for a homogenous family of fluids, inert gases for example, exhibit large deviations when used to model the behavior of other types of fluids (e.g. alkenes, water). These models are of course not usable for mixtures of unlike fluids, e.g. for refrigerants with contaminants. Our selection criteria for appropriate models were as follows:

- The models should be able to predict the speed of sound in mixtures consisting of more than two components.
- The models should not be purely acoustic. In other words, they should also be able to predict vapor-liquid equilibria: the saturation pressure and concentration and the density of both phases.
- The speed-of-sound prediction accuracy both in the liquid phase and in the gas phase should generally be better than 1% in the gas phase and 2% in the liquid phase. This requirement applies to the range of pressures and temperatures that are frequently used in engineering applications for a given fluid or mixture.
- It should be relatively simple to obtain the fitting constant for the model. Ideally, a set of fitting constants for at least some selected fluids should already be available.
- The model should be flexible, i.e. it should be easily applicable to new fluids and mixtures.
- The model must be relatively simple and easy to implement. It should be able to provide a real time calculation, even when implemented in cheap and ubiquitous 32bit microcontrollers (ARM, AVR UC3, ColdFire).

3 Considered models

3.1 Cubic equations of state

Cubic equations might be the first choice. They are well-known and easy to use, and there is an endless list of publications in which cubic equations are applied to various fluids and mixtures. The cubic equations of state generally do well in predicting vapor phase behavior and saturated pressures. Unfortunately, their performance in predicting the liquid phase density and subsequently also the speed of sound is poor for the liquid phase. The deviation from the experimental data is unacceptably high, more than 10% for both properties.

3.2 Virial equations of state

Virial equations of state and acoustic virial equations of state would also be an eligible choice. The coefficients of the acoustic form are related to the coefficients of the classical density form, and can therefore be converted with some effort. Thus the requirement for a speed-of-sound prediction together with the densities and the saturated pressure could be satisfied. The availability of the fitting constants would be also satisfactory, since it is customary to represent experimentally-obtained speed-of-sound data points (surface) with the second and sometimes the third acoustic virial coefficient (which are functions of temperature). Unfortunately, when these coefficients are not already available from well-recognized resources they are difficult to be derive or to obtain. It is necessary to use extremely large datasets containing data points on isotherms.

3.3 Multi-fluid models

Multi-fluid models can combine equations of state in the Helmholtz energy form for different pure fluids into a model that describes a mixture. Perhaps the best known representative of this approach is the GERG (Groupe European de Re-cherches Gazires) model [13], which has been developed for natural gas. The model combines empirical equations of state explicit in the Helmholtz energy of natural gas components such as methane, nitrogen, carbon dioxide, propane, water and others. These individual equations of state are sums of polynomial terms and exponential expressions. The resulting model is very accurate; the claimed uncertainty of speed-of-sound prediction at temperatures above 270 K is 0.2%. This model satisfies most of the criteria mentioned above, with the exception of a low number of the fitting constant and flexibility.

3.4 Acoustic models

The speed-of-sound predictive model by G. Scalabrin et al. [14] is an interesting alternative to the models mentioned above. Although it is an acoustic model which cannot itself be used to predict the vapor liquid equilibrium, it could be used alongside a cubic equation of state that would be used for this purpose, and the model

would be used solely for the speed-of-sound prediction. The model is based on the corresponding state principle, and it requires three fitting parameters. The prediction accuracy of the model was tested on refrigerants (R11, R22, R123, R134a, R143a, and R152a). The average uncertainty of the model is 0.32% in the vapor region and 1.5% in the liquid region. Both numbers are roughly twice as high as the uncertainty of the multiparameter Helmholtz equations of state [22].

4 SAFT equations of state

SAFT models meet our criteria listed in the previous paragraph. The models are developed by applying perturbation theory to the equations of state of a monomer fluid. The added perturbation terms account for chain formation (monomer chains), and additional terms can be added optionally to account for association (hydrogen bonding) or polar molecules. The obtained equations of state are in the Helmholtz energy form, and all thermodynamic properties, including the speed of sound, can be obtained by derivations. The SAFT approach has become quite popular in the last two decades. SAFT equations offer good accuracy for a broad range of fluids, from simple organic or inorganic molecules to complex polymers. A great advantage of these models is the small number of fitting constants; three or four constants are needed for a combination of the monomer term with the chain perturbation, and from five to six constants are needed when the association term is included. Only a small number of vapor pressure data points and saturated liquid density data points are therefore needed in order to obtain the coefficients through the fitting procedure. In addition, a group of contribution methods has been developed for selected SAFT equations of state in order to estimate the coefficients even when no experimental data are available.

A number of publications have dealt with speed-of-sound prediction by various SAFT equations of state. Some comparisons with experimental speed-of-sound data can also be found among evaluations of the prediction accuracy of various thermodynamic properties in papers that present thorough studies of SAFT equations, for example [15]. A smaller number of papers deal only with speed-of-sound predictions, for example [16]. After a thorough study of the available literature and our own data comparisons, three SAFT models were selected for further evaluation: PC-SAFT, Soft-SAFT and SAFT-BACK. It was found later that the performance of the Soft-SAFT equation of state was unsatisfactory, and it was therefore withdrawn from the evaluations presented here. It was also observed that the simplified version of the PC-SAFT equation of state [23] can be used with negligible impact on the results. It is worth mentioning here that a group contribution method has been developed for the sPC-SAFT equation of state [24] that provides a relatively good estimate of the fitting parameters, namely for polymer molecules.

4.1 PC-SAFT

The PC-SAFT equation of state was originally published by Gross and Sadowski [17]. The molecules are assumed to be chains of spheres interacting with the square-well potential. The potential is divided into a reference repulsive part and a perturbation part that accounts for the attractive interactions. The hard-chain fluid is characterized by the sphere-segments diameter σ and by the (average) number of segments in the chain m . The interaction between two chain-like molecules is considered to be the sum of the whole interaction between individual atoms - spherical segments. The chain molecules are also considered to be spherical, and first and second order perturbation terms are used to account for attractive interactions between chain molecules. A simplified version of the original PC-SAFT equation [23] has been used in this paper. The simplified PC-SAFT equation implies that the segment diameters of different species are very similar, and that a simplified radial distribution function can therefore be employed in the chain term. The residual Helmholtz free energy A^{res} consists of two terms (1): the hard-chain reference part A^{hc} and the perturbation part A^{pert} , which is further split into first and second order perturbations A^1, A^2 .

$$A^{res} = A^{hc} + A^{pert} = A^{hc} + A_1 + A_2 \quad (1)$$

The PC-SAFT model uses three fitting parameters:

- σ characterizes the distance of zero potential
- ε characterizes the potential minimum
- m is the number of monomers per chain

Values of the fitting parameters for the fluids investigated in the evaluations presented here are summarized in Table 1.

Table 1. PC-SAFT parameters

	m [-]	σ [Å]	ε/kb [K]
N ₂	1.245	3.293	88.89
C ₃ F ₈	3.332	3.437	153.70
C ₂ F ₆	2.854	3.297	139.33
R22	2.504	3.119	187.70
R23	2.730	2.800	147.49

4.2 SAFT-BACK

The BACK (Boublik–Alder–Chen–Kreglewski) equation of state [18] is an augmented van der Waals equation of state. The equation of state was developed on a statistical description of non-spherical convex molecules. It has been proved that BACK is quite suitable for simple non-associating fluids such as methane, nitrogen, hydrogen and their mixtures. The BACK equation of state provides good prediction even close to the critical point and in the supercritical region. The statistical association fluid theory was applied to this equation to obtain a model for more complex molecules and associating fluids [19]. However, a somewhat different approach was taken, in that the molecules are not

treated as segment-based, as is usually the case with SAFT. Instead, the whole molecule is modelled as a single convex body, and the molecule is modelled as a hard convex body with a dispersion term. For this reason, the SAFT-BACK equation of state is not suitable for long polymer chains. The Helmholtz energy is divided into four parts (2): the hard convex body contribution A^{res} , the chain formation term $A^{chain,hcb}$, the dispersion term A^{dis} and the dispersion due to chain formation $A^{chain,dis}$.

$$A^{res} = A^{hc} + A^{chain,hcb} + A^{dis} + A^{chain,dis} \quad (2)$$

The SAFT-BACK model uses four fitting parameters:

- α geometry of a hard convex body
- m segment number
- u^0 segment dispersion parameter
- v^{00} segment volume parameter

The values of the fitting parameters for the fluids investigated in the evaluations presented here are summarized in Table 2.

Table 2. SAFT-BACK parameters

	m [-]	u^0/k [K]	v^{00} [ml/mol]	α^0 [-]
N ₂	1	128.9	14.02	1.031
C ₃ F ₈	1.647	377.58	29.412	1.072
C ₂ F ₆	1.480	312.73	24.082	1.060
R22	1.364	400.94	18.914	1.081
R23	1.369	334.154	14.712	1.123

4.3 Peng-Robinson equation of state

We have also included the well-known Peng-Robinson cubic equation of state [25] in the evaluations presented in this paper. The Peng-Robinson equation (3) is simple and is popular for engineering applications. It works relatively well for refrigerants, and it can serve as a baseline for comparisons.

$$p = \frac{RT\rho}{1 - b\rho} - \frac{\alpha\rho^2}{1 + 2b\rho - (b\rho)^2} \quad (3)$$

The a , b and α coefficients were evaluated from the critical values listed in Table 3.

Table 3. Critical parameters of the investigated fluids

	T_c [K]	p_c [MPa]	ρ_c [kmol.m ⁻³]
N ₂	126.19	3.396	11.18
C ₃ F ₈	345.02	2.64	3.334
C ₂ F ₆	293.03	3.048	4.44
R22	369.30	4.99	6.0582
R23	299.29	4.832	7.52

5 Ideal gas model

When an equation of state is used (not an acoustic model) the speed of sound, the partial derivation of pressure and both heat capacities are needed. The partial derivation is a function of temperature and density, and the same is the case for the heat capacities and their ratio. The heat capacities again consist of two terms, the ideal part and the residual part, the same way as the Helmholtz energy. The ideal gas heat capacities are related by the well-known relation $C_p - C_v = R$, where R is the ideal gas constant. The ideal gas part of the heat capacity is therefore needed for calculating the speed of sound. It is a function of temperature, and while it can be nearly constant for inert gases such as (Argon and Xenon), the relation between the temperature and the actual ideal gas heat capacity has to be known for fluids such as refrigerants. It is interesting within the scope of this paper that the ideal gas heat capacity values can be determined directly from the measured speed of sound. Datasets measured along isotherms are needed in order to obtain the values of C_p^0 , using the so-called acoustic virial equation of state. For this reason, there is great interest in precise measurements of the speed of sound, and many publications can be found with large datasets of experimentally obtained speed of sound that can be used to evaluate the ideal gas heat capacity. The truncated Einstein term (4) can then be regressed to fit the C_p^0 as a function of temperature.

$$C_p^0 = c_0 + \sum_{i=1}^n b_i \left(\frac{a_i}{T} \right)^2 \frac{\exp\left(\frac{a_i}{T}\right)}{\left[\exp\left(\frac{a_i}{T}\right) - 1 \right]^2} \quad (4)$$

Where the number of fitting constants a_i and b_i is limited to 2 or 3, sacrificing the physical meaning of the coefficients. The first term c_0 is the translational and rotational contribution, and the sum represents the contribution from the vibrational modes. The values of the fitting parameters for the comparisons presented here are provided in Table 4.

Table 4. Ideal gas heat capacity fitting constants

fluid	c_0	a_1/K	a_2/K	a_3/K
N ₂	3.5	0.0011	0.7148	2.3021
C ₃ F ₈	4.0	7.2215	7.2734	11.600
C ₂ F ₆	4.0	2.4806	7.0519	7.9978
R22	4.0	3.1715	4.8343	10.87
R23	4.0	3.0949	2.5237	2.7117
fluid	M [g.mol ⁻¹]	b_1/K	b_2/K	b_3/K
N ₂	188.02	348.56	3223.5	6634.3
C ₃ F ₈	138.01	325.92	595.39	1489.9
C ₂ F ₆	28.01	190.81	621.24	1468.4
R22	86.468	645.68	1660.7	9564
R23	70.014	2074.8	757.75	1468.2

6 Calculating the speed of sound

The first and second order derivatives of Helmholtz free energy are needed in order to obtain thermodynamic properties such as pressure, heat capacities and others. Derivatives of both the ideal gas Helmholtz free energy and the residual Helmholtz free energy equations have to be combined in order to obtain a complete thermodynamic model. The well-known equation (5) is used to calculate the speed of sound.

$$u = \sqrt{\frac{c_p}{c_v} \left(\frac{\partial p}{\partial \rho} \right)_T} \quad (5)$$

Both the heat capacities and the pressure are derived from the Helmholtz equations, and they are functions of density and temperature. With some fluids, variations in the measured speed of sound can be observed for different sound frequencies. This is due to the frequency dependence of the specific heat capacity, which is explained by phenomena referred to as molecular relaxation. The heat capacity C consists of the rotational, vibrational and translation modes (6).

$$C = C^{rot} + C^{vib} + C^{trans} \quad (6)$$

After the gas is excited by the travelling sound wave, the times for the modes to come back to equilibrium are different. The relaxation time τ of the vibrational energy is much longer than the other modes, and it can be up to 10⁻⁴ seconds. Dispersion can therefore be observed at sound frequencies above $1/\tau$, where the rotational contribution approaches zero. For slowly relaxing gases (high τ) the dispersion is measurable even at acoustic frequencies. To account for the relaxation, corrected effective values of heat capacities C^{eff} are used (7).

$$C^{eff} = C^{trans} + C^{rot} + \frac{C^{vib}}{1 + i\omega\tau} \quad (7)$$

Note that C^{eff} is a complex number, and the real part is the effective heat capacity to be used to evaluate the speed of sound. At high frequencies $\omega = 2\pi f$ the effective value is equal only to the translational and rotational contribution. When a sufficiently low frequency, below the reciprocal of the relaxation time, is used for measuring the speed of sound, the dispersion is negligible. Carbon dioxide and methane are two examples of slowly relaxing gases. Apart from speed dispersion, they also exhibit strong sound attenuation. The relaxation times of fluorocarbon refrigerant are usually tens of nanoseconds, and no correction to the speed of sound due to molecular relaxation was applied in the evaluation presented here.

7 Speed of sound measurement

Numerous speed-of-sound measurement methods have been perfected in the past century. The main reason is that very high-quality data are needed to derive other thermodynamic properties, such as the essential ideal gas heat capacity, as mentioned above. Three main

measurement principles are used nowadays:

- Resonance
- Interferometers
- Time-of-flight

The spherical resonator, the cylindrical resonator and the annular resonator are the most widely-used instruments for methods based on resonance. Cylindrical resonators offer the best accuracy available today. The uncertainty of the speed of sound that is obtained can be as small as 0.01% or 0.0001%, when the results are corrected for known sources of error [21]. The main disadvantage of spherical resonators is that the measurement cavity is difficult to manufacture, and is therefore expensive. Cylindrical resonators are a somewhat cheaper alternative with less accuracy. Resonant methods are based on measuring the response to a frequency sweep of a cavity filled with gas that is under observation. The speed of sound is then determined from the resonant peaks obtained in the response.

Interferometers are similar to cylindrical resonators, except that the excitation frequency is fixed while the length of the cylindrical cavity is variable. The advantages and drawbacks are obvious: some means of precise positioning is needed, and this renders automated measurement quite complicated and slow, while, on the other hand, transducers operate at a fixed frequency, so that narrow-bandwidth types are sufficient.

Time-of-flight methods are very simple, and require only relatively cheap instrumentation. This method is very widely-used for the liquid phase, while precise measurements in the gas phase require transducers with high sensitivity on acceptance. Since industrial ultrasonic flowmeters are based on time-of-flight measurements, they can be used to obtain the speed of sound for fluid analysis. The accuracy of a simple time-of-flight measurement can be well below 1%, especially after calibration [20].

In all cases, some type of acoustic transducer is needed to translate sound energy to electrical energy, and vice versa. The most widely-used types are:

- piezoelectric transducers
- capacitive transducers

A broad range of piezoelectric transducers are commercially available nowadays. They have relatively low sensitivity on acceptance and narrow band frequency characteristics. They are ideally suitable for time-of-flight measurements in liquids, but are much less suitable for gases. A so-called matching layer is used to improve the performance and the energy losses on the transducer-gas interface. Capacitive transducers have high sensitivity and a flat frequency response. Unfortunately, only a small number of models are commercially available.

8 Experimental setup

We constructed an apparatus for speed-of-sound measurements in gases in order to gather new and unique data for two little-used refrigerants and their mutual mixtures and mixtures with nitrogen. The apparatus is

based on time-of-flight measurements; it uses capacitive transducers operated at 50 kHz. The temperature of the measured gas can be controlled, and the data point collection is automated. As a result, measurements can be carried out both on isotherms and on isochors. The typical temperature and pressure range for the measurements is from -20°C to $+50^{\circ}\text{C}$, and from 0.02 MPa up to 0.5 MPa. When the measured fluid exhibits a phase transition within these limits, the setup can be used to investigate the saturation curve. The arrangement of the apparatus is shown in Figure 5. A pair of capacitive ultrasound transducers, facing each other, is placed inside a tube-like stainless steel pressure vessel. In general, one transducer transmits a short burst of ultrasound pulses while the second transducer acts as a receiver. A 20 MHz clock is used to measure the time of flight, and a high-speed amplifier and trigger circuits are used to minimize the trigger delays, Figure 6.

The distance between the diaphragms of the transducers has to be fixed and has to be well known. The exact distance as a function of temperature was obtained from calibration with Nitrogen, and the following equation was obtained by regression with uncertainty of 0.4%:

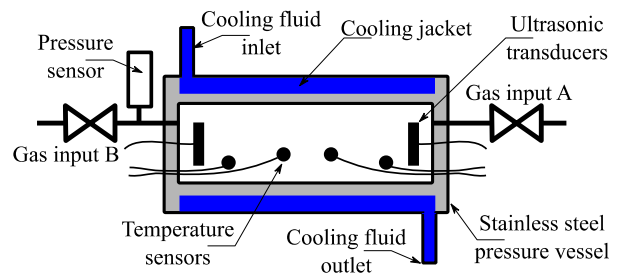


Figure 5. Speed-of-sound measurement apparatus

Glycol from a chiller unit circulates in the double jacket of the vessel, keeping the gas at the desired temperature. The flanges on the end of the tube are equipped with several ports for vacuum and for the measured gas, and also with sealing bulkhead electrical connectors. Several temperature sensors installed inside the pressure vessel are wired to these connectors together with the transducers. These sensors are evenly arranged, so that they measure the temperature along the sound path. A precise pressure sensor monitors the pressure during the measurement.

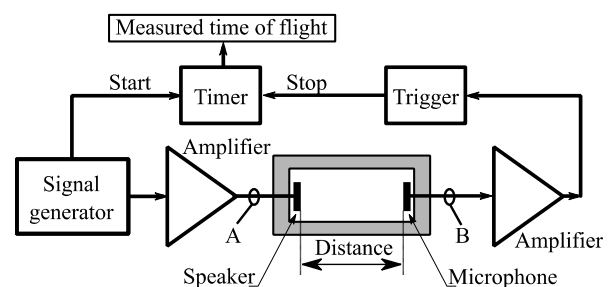


Figure 6. Time-of-flight measurement electronics

The uncertainty of the obtained speed of sound was determined to be 0.4%. This value is predominantly due to the uncertainty of the calibrated distance. Although the uncertainty of the temperature measurement is small, a measurement error is introduced by the inhomogeneity of the temperature distribution inside the pressure vessel. We reduced this error by using six internal sensors. However, the error is still smallest when the measurement is carried out at the ambient temperature, and it increases with both higher and lower temperatures. The temperature distribution inside the measurement cell becomes less homogenous with increasing difference between the measurement temperature and the room ambient temperature, in spite of the decent insulation. The measurement uncertainties are summarized in Table 5.

Table 5. Measurement uncertainties

Pressure	300	[Pa]
Temperature	0.1	[°C]
Speed of sound	0.4	[%]

9 Experimental data

We have obtained data for pure C_3F_8 and C_2F_6 , their mutual mixture (5.4% of C_2F_6) and a mixture consisting of C_3F_8 and 6.3% of Nitrogen. On average, more than 330 data points were measured for each fluid. The acquired data for pure fluids are shown in Figure 8 and Figure 9. It can be seen that the speed of sound data points measured with the pure C_3F_8 were very close to the saturation curve (solid line). A phase transition (condensation) occurred during the measurement cycle, and the corresponding data points were omitted. The pressure and temperature ranges of the acquired data are from 0.06 MPa absolute to 0.3 MPa absolute, and from -22°C to $+52^\circ\text{C}$. Each data point was acquired twice, once in a measurement cycle with increasing temperature and then during a cycle with decreasing temperature. Fifteen isotherms were obtained for each fluid. The standard deviation of the data point temperatures on each of the isotherms was lower than 0.052 K.

As is customary, the measured data were correlated with the acoustic virial equation (8).

$$u^2 = \frac{\gamma^{id} RT}{M} \{1 + B_a \rho\} \quad (8)$$

A value of the first acoustic virial coefficient B_a was obtained for each isotherm. The resulting correlations are shown in Table 6 and in Figure 7.

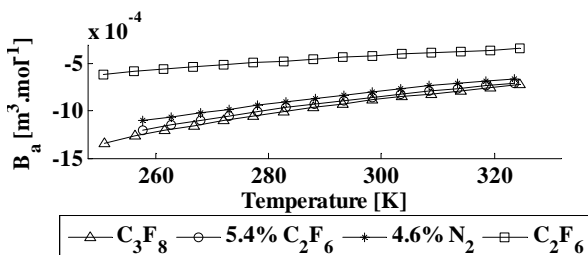


Figure 7. Regressed acoustic virial coefficients

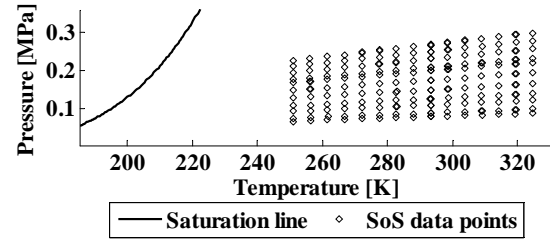


Figure 8. Measured speed of sound data for C_2F_6

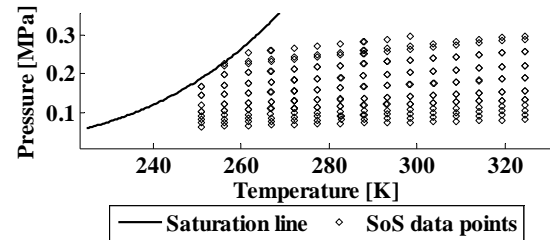


Figure 9. Measured speed of sound data for C_3F_8

Table 6. Regressed acoustic virial coefficients

T [K]	B_a [$10^6 \text{m}^3 \cdot \text{mol}^{-1}$]			
	C_3F_8	C_2F_6	5.4% C_2F_6	4.6% N_2
252.0	-1327.3	-606.67		
262.0	-1206	-558.23	-1157.7	-1072.5
272.0	-1103.8	-515.18	-1062.9	-992.05
282.0	-1014.2	-476.14	-977.5	-912.21
292.0	-934.34	-440.73	-900.65	-840.92
302.0	-863.47	-408.81	-831.93	-777.08
312.0	-800.33	-379.79	-770.7	-717.73
322.0	-741.14	-351.99	-715.84	-665.26
AAD	0.96	0.87	0.77	1.33

10 Evaluation of the results

Our own speed of sound data for pure C_2F_6 vapor were further extended by a dataset measured with a cylindrical resonator, adopted from [27]. To our knowledge, no data are available for the liquid phase of C_3F_8 or C_2F_6 . Speed-of-sound data for pure nitrogen from a spherical resonator were adopted from [26]. Both liquid-phase and vapor-phase data for R22 and R23 refrigerants were also included in the evaluation in order to provide a comprehensive study. The vapor phase data for R22 measured with a spherical resonator were adopted from [28], while the vapor phase data for R23 measured with an annular resonator originates from [30]. The speed of sound data measured in the liquid phase of R22 with an ultrasonic interferometer were adopted from [29] and the data for the liquid phase of R23 measured with the pulse-echo method come from [31]. The temperature and pressure ranges of the measurements are summarized in

Table 7. The uncertainty of the speed of sound in the adopted data containing vapor measurement is better than 0.04%, with the exception of the data for C_2F_6 , where the uncertainty is 0.5%. The liquid phase measurement uncertainty is somewhat higher, 0.4%.

All the data sets include temperature, pressure and speed of sound values. In order to compare them with the presented models, the first step is to determine the density from the pressure and temperature, and only then can the speed of sound be calculated. This means that the resulting deviation of the speed of sound is also affected by the uncertainty of the temperature and pressure. The uncertainty of the temperature measurement is better than 0.03 K in all adopted data sets. The uncertainty of the pressure measurement varies significantly, especially for the measurements with liquids, which were carried out up to very high pressures. In general, the pressure uncertainty in the adopted measurements with vapors is 0.06%, except in the case of R22, for which the pressure uncertainty is 1%. The pressure uncertainty for liquids is below 3%.

The resulting average deviation between the data and the models given in Table 8 was calculated as follows:

$$AD = 100 \frac{1}{n} \sum_{i=1}^n \frac{|x_i^{fit} - x_i^{measured}|}{x_i^{measured}} [\%] \quad (9)$$

Selected representative results are plotted in Figure 10, Figure 11 and Figure 12. The difference between the predicted speed of sound and the measured speed of sound in the vapor phase increases with density. Note the poor prediction of the Peng-Robinson equation of state in the liquid phase, Figure 12.

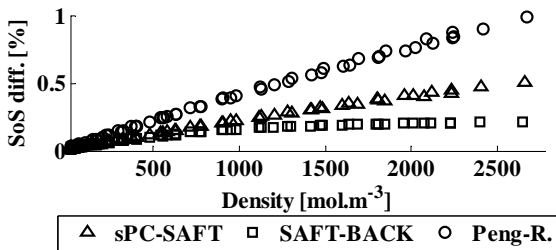


Figure 10. Results for the nitrogen

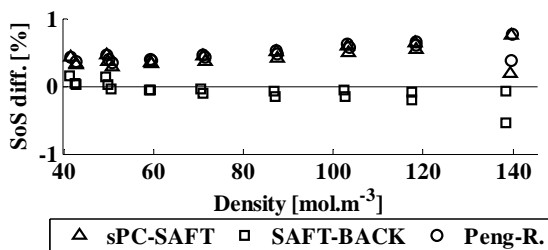


Figure 11. Results for the $C_3F_8+C_2F_6$ mixture (a reduced number of data points are shown)

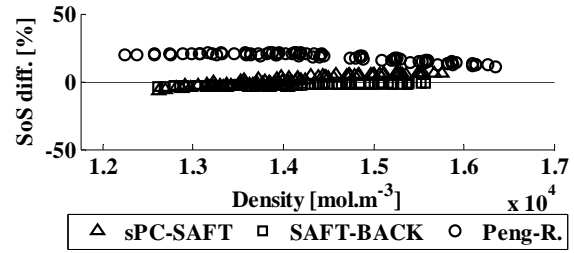


Figure 12. Results for the R22 liquid

Table 7. Sources and ranges of collected data

Fluid	Temp. range		Pressure range	
	[K]	[K]	[MPa]	[MPa]
N_2 vapor [26]	296	325	0.049	6.639
C_2F_6 vapor	251	325	0.059	0.297
C_2F_6 vapor [27]	210	475	0.100	1.505
C_3F_8 vapor	251	325	0.062	0.299
$C_3F_8+C_2F_6$ vap.	253	324	0.087	0.352
$C_3F_8+N_2$ vap.	253	324	0.086	0.370
R22 vapor [28]	294	323	0.199	0.6490
R22 liquid [29]	293	323	0.788	51.20
R23 vapor [30]	297	297	1.628	4.369
R23 liquid [31]	258	298	2.540	65.420

Table 8. Deviations of models from data

Fluid	Data points	Average deviation		
		sPC [%]	SB [%]	PR [%]
N_2 vapor [26]	70	0.18	0.12	0.34
C_2F_6 vapor	341	0.38	0.14	0.42
C_2F_6 vapor [27]	171	0.54	0.14	0.49
C_3F_8 vapor	355	0.34	0.15	0.37
$C_3F_8+C_2F_6$ vap.	244	0.43	0.13	0.48
$C_3F_8+N_2$ vap.	432	0.39	0.11	0.32
R22 vapor [28]	24	0.11	0.13	0.45
R22 liquid [29]	157	3.31	2.44	18.07
R23 vapor [30]	9	3.67	1.09	3.51
R23 liquid [31]	185	9.28	5.80	10.99
Average deviation vapor		0.76	0.25	0.80
Average deviation liquid		6.29	4.12	14.53

11 Conclusions

It is immediately apparent from the results summarized in Table 8 that the SAFT-BACK model exhibits the best agreement both in the vapor phase and in the liquid phase. Disregarding the deviation for the R23 refrigerant, the SAFT-BACK model agrees with the vapor phase experimental data within 0.13%. This is better

agreement than the average deviations reported for the acoustic model by G. Scalabrin et al. [14]. PC-SAFT shows roughly twice as high deviation. The results for both phases of the R23 refrigerant show noticeably high deviations for all three models. However, a similar pattern in the performance of the particular models is apparent.

It is worth noting that the deviations of the models from the data measured with our own apparatus are in line with the adopted vapor phase data, which were measured with resonators. This provides confirmation that the time-of-flight measurement method is suitable for obtaining high-quality speed-of-sound measurements.

The poor accuracy of the Peng-Robinson equation of state in the liquid phase provides further confirmation of the unsuitability of cubic equations-of-state for tasks related to refrigerants and their mixtures. Although the SAFT-BACK model has the smallest deviation from the liquid data for the R22 refrigerant, the actual value is still relatively high. It has also been shown that the speed-of-sound prediction accuracy of the SAFT models in the liquid phase can be further improved by modifying the model constants, i.e. the constants used in the equations, but not the fitting constants for fluids [15].

Nomenclature

α	Peng-Robinson coefficient ($\text{mol}\cdot\text{m}^{-3}$)
γ	Poisson constant (-)
ρ	density ($\text{mol}\cdot\text{m}^{-3}$)
ω	frequency (-)
a	constant (-)
b	constant (-)
n	number of measured data point (-)
p	pressure (MPa)
t	relaxation time (s)
u	speed of sound (m s^{-1})
x	measured value (-)
A	Helmholtz energy (J)
B_a	second acoustic virial coefficient ($\text{m}^3\cdot\text{mol}^{-1}$)
C	heat capacity ($\text{J mol}^{-1} \text{K}^{-1}$)
C_p	heat capacity at constant pressure ($\text{J mol}^{-1} \text{K}^{-1}$)
C_v	heat capacity at constant volume ($\text{J mol}^{-1} \text{K}^{-1}$)
R	universal gas constant ($\text{J mol}^{-1} \text{K}^{-1}$)
T	temperature (K)

References

- [1] M. Guangtian, A. J. Jaworski, N. M. White, Composition measurements of crude oil and process water emulsions using thickfilm ultrasonic transducers, *Chemical Engineering and Processing: Process Intensification*, Volume 45, Issue 5, May 2006, Pages 383-391, ISSN 0255-2701, <http://dx.doi.org/10.1016/j.cep.2005.10.004>.
- [2] W. Schaik M. Grooten, T. Wernaart, C. Geld, High Accuracy Acoustic Relative Humidity Measurement in Duct Flow with Air. *Sensors* 2010, 10, 7421-7433. doi:10.3390/s100807421
- [3] Zhan Tung-Sheng, Wu Sun-Li, Tsai Wen-Yuan, Spontaneous and highly accurate ultrasonic temperature measurement system for air conditioner in automobiles, *JSIR* Vol.68(01), January 2009
- [4] J. J. Baustian, Development of a sensor for the continuous measurement of oil concentration in a refrigeration system, 1988, Retrospective Theses and Dissertations, Paper 9327. <http://lib.dr.iastate.edu/rtd/9327>
- [5] H. Tahani, Determination of the Velocity of Sound in Reservoir Fluids Using an Equation of State, 2011 Heriot-Watt University, Institute of Petroleum Engineering
- [6] R. King, M. Bretland, A. Wilkes, J. Dingley, Xenon measurement in breathing systems: a comparison of ultrasonic and thermal conductivity methods, *Anaesthesia*. 2005 Dec, 60(12):1226-30.
- [7] M. Dekker, *Engineering Properties of Food*, Second Edition, 1994 Volume 63 of Food Science and Technology, CRC Press, ISBN 0824789431,
- [8] A. Petculescu, P. Achi, A model for the vertical sound speed and absorption profiles in Titan's atmosphere based on Cassini-Huygens data. *Journal of the Acoustical Society of America*, 131, 3671-3679 (2012), DOI:<http://dx.doi.org/10.1121/1.3699217>
- [9] 8500 Series - Binary Liquid Analysers, 2016, April 7, Retrieved from <http://www.rhosonics.nl/models/8500>
- [10] TTP Press Release SonicSense, 2016, April 7, Retrieved from http://www.ttp.com/news/2014/01/sonic_sense
- [11] A combined ultrasonic flow meter and binary vapour mixture analyzer for the ATLAS silicon tracker, *Journal of Instrumentation*, Vol 8, doi:10.1088/1748-0221/8/02/P02006
- [12] E.W Lemmon, .M. L. Huber, M.O. McLinden, NIST Standard Reference Database 23: Reference Fluid Thermodynamic and Transport Properties-REFPROP, Version 9.1, National Institute of Standards and Technology, Standard Reference Data Program, Gaithersburg, 2013.
- [13] O. Kunz and W. Wagner, The GERG-2008 Wide-Range Equation of State for Natural Gases and Other Mixtures: An Expansion of GERG-2004, *Journal of Chemical & Engineering Data* 2012 57 (11), 3032-3091, DOI: 10.1021/je300655b
- [14] G. Scalabrin, P. Marchi, M. Grigiante, Speed of sound predictive modeling in a three-parameter corresponding states format: Application to pure and mixed haloalkanes, *Experimental Thermal and Fluid Science*, Volume 31, Issue 3, January 2007, Pages 261-278, ISSN 0894-1777, <http://dx.doi.org/10.1016/j.expthermflusci.2006.04.006>.
- [15] X. Liang, B. Maribo-Mogensen, K. Thomsen, W. Yan, G. M. Kontogeorgis, Approach to Improve Speed of Sound Calculation within PC-SAFT Framework, *Industrial & Engineering Chemistry Research* 2012 51 (45), 14903-14914, DOI: 10.1021/ie3018127
- [16] T. Lafitte, A. Apostolou, C. Avendaño, A. Galindo, C. S. Adjiman, E. A. Müller, G. Jackson, Accurate statistical associating fluid theory for chain molecules formed from Mie segments, *The Journal of Chemical Physics*, 139, 154504 (2013), DOI:<http://dx.doi.org/10.1063/1.4819786>
- [17] J. Gross, G. Sadowski, Perturbed-Chain SAFT: An Equation of State Based on a Perturbation Theory for Chain Molecules, *Industrial & Engineering Chemistry Research* 2001 40 (4), 1244-1260, DOI: 10.1021/ie0003887
- [18] T. Boublik, BACK equation of state for simple compounds, *Journal of Molecular Liquids*, Volume 134, Issues 1-3, 15 May 2007, Pages 151-155, ISSN 0167-7322, <http://dx.doi.org/10.1016/j.molliq.2006.12.008>.
- [19] Zhi-Yu Zhang, Ji-Chu Yang, Yi-Gui Li, The use of statistical associating fluid theory to improve the BACK equation of state: I. Pure fluids, *Fluid Phase Equilibria*, Volume 172, Issue 2, 5 July 2000, Pages 111-127, ISSN 0378-3812, [http://dx.doi.org/10.1016/S0378-3812\(00\)00386-1](http://dx.doi.org/10.1016/S0378-3812(00)00386-1).
- [20] V. Vacek, M. Vitek, M. Doubek, Velocity of sound in Per-

- fluoropropane (C3F8), Perfluoroethane (C2F6) and their mixtures, *Fluid Phase Equilibria*, Volume 351, 15 August 2013, Pages 53-60, ISSN 0378-3812, <http://dx.doi.org/10.1016/j.fluid.2012.10.002>.
- [21] A. R. H. Goodwin, K.N. Marsh, and W. A. Wakeham, editors. Measurement of the thermodynamic properties of single phases, volume VI of *Experimental Thermodynamics*. Elsevier, 2003. ISBN 0-444-50931-3
- [22] E. W. Lemmon, R. Span, Short Fundamental Equations of State for 20 Industrial Fluids, *Journal of Chemical & Engineering Data* 2006 51 (3), 785-850, DOI: 10.1021/je050186n
- [23] G. M. Kontogeorgis, N. Solms, M. L. Michelsen, L. Constantinou, Capabilities, limitations and challenges of a simplified PC-SAFT equation of state, *Fluid Phase Equilibria*, Volume 241, Issues 1-2, 15 March 2006, Pages 344-353, ISSN 0378-3812, <http://dx.doi.org/10.1016/j.fluid.2006.01.001>.
- [24] A. Tihic, G. M. Kontogeorgis, N. Solms, M. L. Michelsen, L. Constantinou, A Predictive Group-Contribution Simplified PC-SAFT Equation of State: Application to Polymer Systems, *Industrial & Engineering Chemistry Research* 2008 47 (15), 5092-5101, DOI: 10.1021/ie0710768
- [25] D.Y. Peng and D. B. Robinson, A New Two-Constant Equation of State, *Ind. Eng. Chem., Fundam.*, Vol. 15, No. 1, 1976
- [26] S. J. Boyes, The speed of sound in gases with application to equations of state and sonic nozzles, February 1992, A thesis submitted to the University of London for the Degree of Doctor of Philosophy, University of London, Department of Chemistry, <http://discovery.ucl.ac.uk/id/eprint/1317924>
- [27] J. J. Hurly, Thermophysical Properties of Gaseous CF4 and C2F6 from Speed-of-Sound Measurements, 1999, *International Journal of Thermophysics*, Vol. 20, No. 2, doi:10.1007/s10765-005-0001-6
- [28] M. G. He, Z. G. Liu, J. M. Yin, Measurement of Speed of Sound with a Spherical Resonator: HCFC-22, HFC-152a, HFC-143a and Propane, November 2002, *International Journal of Thermophysics* Vol. 23 No.6, doi: 10.1023/A:1020742018220
- [29] Toshiharu Takagi, and Hiroshi Teranishi, Ultrasonic Speeds in Liquid Monochlorodifluoromethane (R22) and Monochloropentafluoroethane (R115) under High Pressures, 1988, *J. Chem. Eng. Data* 33 169-173, doi:10.1021/je00052a033
- [30] G. K. Jarvis, K. A. Johnson, S. L. Walmsley, An Annular Resonator Used To Measure the Speed of Sound in Gaseous Fluoroalkanes: Trifluoromethane and Hexafluoroethane, 1996, *Journal of Chemical and Engineering Data* Vol. 41 No. 2, doi:10.1021/je950231z
- [31] P. F. Pires, H. J. R. Guedesa, The speed of sound, and derived thermodynamic properties of liquid trifluoromethane (HFC23) from T = (258 to 303) K at pressures up to 65 MPa, 1999, *J. Chem. Thermodynamics* 31 479-490, doi:10.1006/jcht.1998.0464